



# Study of Mg–Gd–Zn–Zr alloys with long period stacking ordered structures

Jinshan Zhang\*, Wenbo Zhang, Liping Bian, Weili Cheng, Xiaofeng Niu, Chunxiang Xu, Shaojie Wu

College of Materials Science and Engineering, Taiyuan University of Technology, Taiyuan 030024, China

## ARTICLE INFO

### Article history:

Received 4 April 2013

Received in revised form

9 July 2013

Accepted 11 July 2013

Available online 31 July 2013

### Keywords:

Long period stacking ordered (LPSO)

structures

Equal channel angular pressing (ECAP)

Mg–Gd–Zn–Zr alloys

Mechanical properties

## ABSTRACT

The microstructure evolution of  $\text{Mg}_{96-x}\text{Gd}_3\text{Zn}_1\text{Zr}_x$  (at%) ( $x=0, 0.1, 0.2, 0.4$ ) alloys with long period stacking ordered (LPSO) structures prepared by conventional permanent mold casting were investigated by XRD, EDS, SEM and TEM. Also, the deformation behavior and microstructure evolution of  $\text{Mg}_{95.8}\text{Gd}_3\text{Zn}_1\text{Zr}_{0.2}$  (at %) alloy subjected to equal channel angular pressing (ECAP) were examined. The results show that the LPSO structure phases observed in as-cast  $\text{Mg}_{96}\text{Gd}_3\text{Zn}_1$  alloy did not notably improve the mechanical properties of the alloy owing to their low volume fraction. In contrast, the mechanical properties of the alloy after heat treatment were raised significantly because of the transformation from eutectic structures to LPSO structure phases. Furthermore, moderate Zr addition into Mg–Gd–Zn alloys refined and homogenized  $\alpha$ -Mg grains, changed the morphology and distribution of LPSO structure phases and promoted the precipitation of strengthening phases, and hence strengthened the alloys. Besides, tensile test results showed that aging-treated  $\text{Mg}_{95.8}\text{Gd}_3\text{Zn}_1\text{Zr}_{0.2}$  alloy subjected to 2-pass ECAP processing exhibited high ultimate tensile strength (UTS) of 418 MPa, yield strength (YS) of 330 MPa and elongation of 7.5%. Such excellent mechanical properties could be attributed to complex strengthening of kinking LPSO phases and the dispersion strengthening of tiny spherical phases.

© 2013 Elsevier B.V. All rights reserved.

## 1. Introduction

Magnesium (Mg) alloys, as the lightest metallic structural materials, have attracted great attention because of their low density, high specific strength, good damping capacity and easy recycling [1–3]. However, the inherently weak properties of Mg alloys, such as low strength, inferior ductility and poor thermal stability, seriously limit their wide applications in engineering. In the last decade, the strength and the ductility of Mg alloys have exhibited great improvement benefited from the discovery of LPSO structures phases, which indicates a bright prospect of Mg alloys in engineering [4–14].

Kawamura researched the formation of LPSO structures in  $\text{Mg}_{97}\text{Zn}_2\text{RE}_1$  (at%) alloys, considered Mg–Gd–Zn as the type II alloys, in which the LPSO phases were nonexistent in as-cast ingots but precipitated with soaking at 773 K [15]. However, Wu found 14H-LPSO structures in as-cast Mg–Gd–Zn alloys [16]. About the effect of Zr on Mg alloys, Qian reported that Zr refined the alloys by promoting nucleation as heterogeneous nucleation cores [17]. And Zeng obtained  $\text{Mg}_{96.32}\text{Gd}_{2.5}\text{Zn}_1\text{Zr}_{0.18}$  (at%) alloys with UTS=290 MPa, YS=162 MPa,  $\delta=10.35\%$  [18]. Shao [19] and Yamasaki [20]

studied the deformation behavior of Mg–Zn–Y and Mg–Zn–Gd alloys during extrusion and obtained excellent mechanical properties, which were attributed to the LPSO phases and the fine microstructures.

However, there was little study on Zr-containing LPSO Mg alloys. Especially, no details about the effect of Zr on the formation and transformation of LPSO phases were reported by now. In order to clarify the effect of Zr on the strengthening of LPSO phases,  $\text{Mg}_{96-x}\text{Gd}_3\text{Zn}_1\text{Zr}_x$  (at%) ( $x=0, 0.1, 0.2, 0.4$ ) alloys under different heat treatment conditions and equal channel angular pressing (ECAP) processed condition were investigated.

## 2. Experimental procedures

$\text{Mg}_{96-x}\text{Gd}_3\text{Zn}_1\text{Zr}_x$  alloys (at%) ( $x=0, 0.1, 0.2$  and  $0.4$ ) named as alloys A, B, C and D respectively were prepared by using high-purity Mg, Zn, Gd and Mg–30Zr (wt%) master alloy through induction melting in a mild steel crucible under a mixed protective gas atmosphere of  $\text{CH}_2\text{FCF}_3$  (2.6 vol%) and  $\text{N}_2$  (97.4 vol%) at 1033 K. Then they were cast into a preheated mold at 993 K. The as-cast alloys were performed by solid solution treatment at 773 K for 50 h and aging-treated at 473 K for 80 h in a SX2-8-10 box type high-temperature electric resistance furnace, followed by water quenching. The samples

\* Corresponding author. Tel./fax: +86 351 601 8208.

E-mail address: [jinshansx@tom.com](mailto:jinshansx@tom.com) (J. Zhang).

for ECAP processing were taken from the cast ingot with the dimensions of  $10 \times 10 \times 50 \text{ mm}^3$ . ECAP process was performed using a die with  $\varphi=90^\circ$  (inner arc of curvature) and  $\psi=20^\circ$  (outer arc of curvature). The samples were subjected to 1 and 2 passes of ECAP at 603 K with an extrusion speed of 2 mm/min. Then the tensile specimens with a gauge dimension of  $18 \text{ mm} \times 4 \text{ mm} \times 2 \text{ mm}$  were cut from the ECAP processed samples. Tensile tests were performed by a DNS100 electronic universal material test machine with an initial strain rate of  $3.33 \times 10^{-4} \text{ s}^{-1}$  at ambient temperature. Microhardness was measured by a HVS-1000A Vikers hardness testing machine, with load of 10 g and loading time of 15 s. Brinell hardness was measured by a HB-3000 Brinell hardness testing machine with a load of 62.5 kg and loading time of 15 s. Phase constitute analysis was performed with Y-2000 X-ray diffraction (XRD), using monochromatic Cu-K $\alpha$  radiation. The microstructures and compositions of different phases in the alloys were investigated by scanning electron microscopy (SEM, JSU-6700F) equipped with energy dispersive spectroscopy (EDS) and transmission electron microscopy (TEM, JEOL 2010). Thin foils for TEM observation were prepared by cutting the bulk sample into slices, grinding to the thickness of about 50  $\mu\text{m}$ , and ion milling finally.

### 3. Results and discussion

#### 3.1. Microstructures of as-cast alloys A, B, C, and D

Fig. 1 shows the optical microstructures (OM) of alloys A, B, C, and D respectively. White  $\alpha$ -Mg matrix and black eutectic structure  $\beta$ -(Mg, Zn) $_3$ Gd phases [18] which located at the boundaries of grains

were observed. However, the different additions of Zr led to various morphologies of eutectic structure, which indicated that Zr addition affected the growth patterns of the  $\alpha$ -Mg grains. In the Zr-free alloy A, coarse dendrite was observed (as shown in Fig. 1a). While the  $\alpha$ -Mg grains were close to spherical shape with a smaller grain size after 0.1% Zr addition (Fig. 1b). When 0.2% Zr was added, homogeneous spherical grains with an average grain size of 24  $\mu\text{m}$  were observed in alloy C (Fig. 1c). And when Zr content was up to 0.4%, smaller spherical  $\alpha$ -Mg grains with the average grain size of about 20  $\mu\text{m}$  (as shown in Fig. 1d) were obtained in alloy D.

In order to clarify the reason why homogeneous spherical grains were formed after the Zr addition, electron back-scattering diffraction (EBSD) was carried out about the alloy C. As shown in Fig. 2a, tiny bright phases were observed in the center of spherical grains. The line scanning result (Fig. 2b) revealed the tiny bright phases were Zr-rich cores, which was consistent with the report by Qian [17]. It is clear that Zr-rich phases as heterogeneous nucleation cores promoted the nucleation of  $\alpha$ -Mg grains and refined the matrix grains. Therefore, smaller grain size contributed to higher strength of the alloy according to Hall–Petch relationship. In addition, homogeneous grain structure avoided the stress concentration and thus promoted strengthening effect.

As shown in the bright field (BF) TEM image of as-cast alloy A (Fig. 2c), besides the eutectic structures, some lamellar phases were observed in Mg matrix, which were also observed in as-cast alloys B, C, and D. Fig. 2d is the high magnification image and the corresponding selected area electron diffraction (SAED) patterns of lamellar phases. Small periodic diffraction spots at the interval of  $1/14$  of distance between direct spot and  $(0002)_{\text{Mg}}$  reflection were observed, the spot of  $(00014)$  corresponded to that of  $(0002)_{\text{Mg}}$ .

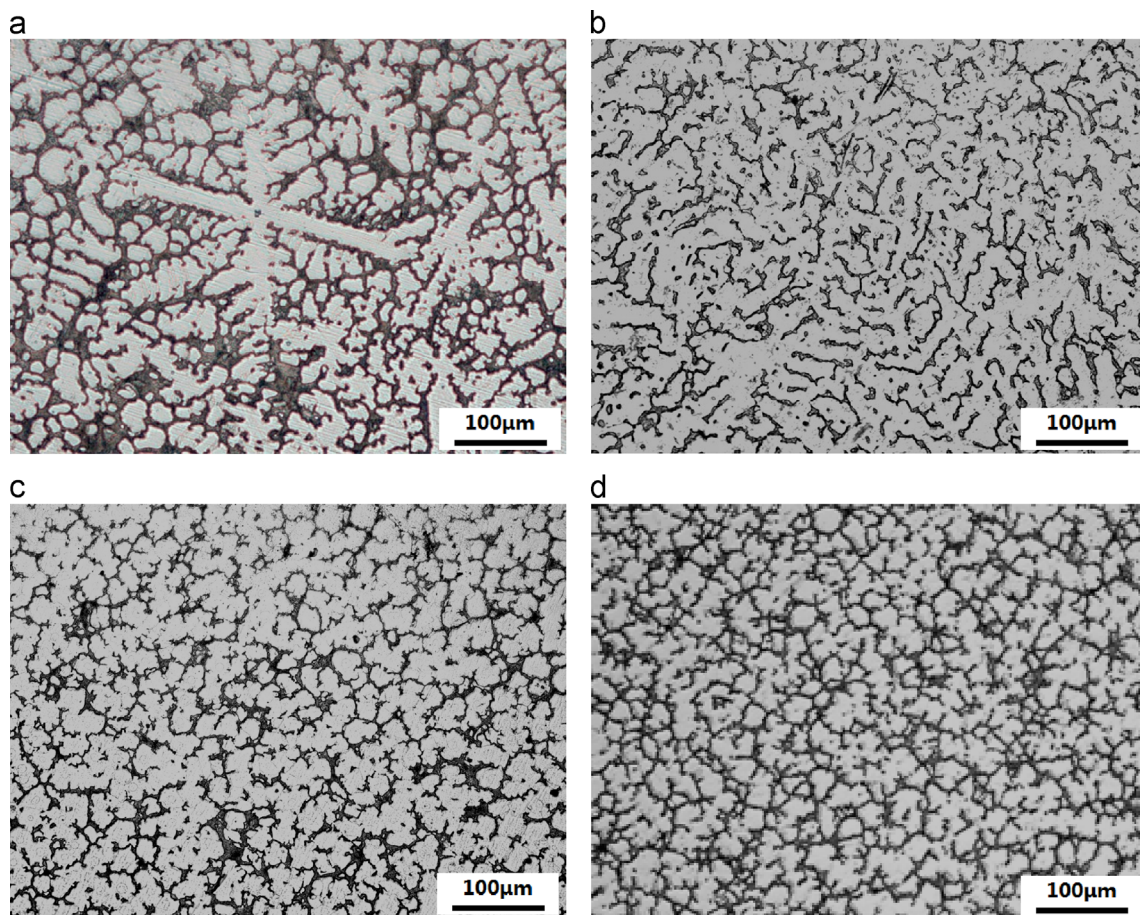


Fig. 1. OM images of as-cast (a) alloy A, (b) alloy B, (c) alloy C, and (d) alloy D.

Download English Version:

<https://daneshyari.com/en/article/7982571>

Download Persian Version:

<https://daneshyari.com/article/7982571>

[Daneshyari.com](https://daneshyari.com)